International Journal of Water Resources and Environmental Engineering

Volume 8 Number 3 April 2016

ISSN-2141-6613

Academic Journals

www.academicjournals.org/ijwree

ABOUT IJWREE

The International Journal of Water Resources and Environmental Engineering is published monthly (one volume per year) by Academic Journals.

International Journal of Water Resources and Environmental Engineering (IJWREE) is an open access journal that provides rapid publication (monthly) of articles in all areas of the subject such as water resources management, waste management, ozone depletion, Kinetic Processes in Materials, strength of building materials, global warming etc. The Journal welcomes the submission of manuscripts that meet the general criteria of significance and scientific excellence. Papers will be published shortly after acceptance. All articles published in IJWREE are peer-reviewed.

Contact Us

Editorial Office: ijwree@academicjournals.org

Help Desk: helpdesk@academicjournals.org

Website: http://www.academicjournals.org/journal/IJWREE

Submit manuscript online http://ms.academicjournals.me/

International Journal of Water Resources and Environmental Engineering

Table of Contents: Volume 8 Number 3 April 2016

ARTICLES

academicJournals

Vol. 8(3), pp. 32-38, April 2016
DOI: 10.5897/IJWREE2015.0627
Article Number: 9E3D63F58102
ISSN 2141-6613

http://www.academicjournals.org/IJWREE

International Journal of Water Resources and Environmental Engineering

Full Length Research Paper

Continuous and stochastic methods for modeling rain drop growth in clouds

Rehan Siddiqui[1]* and Brendan M. Quine[1, 2]

[1]Department of Physics and Astronomy, York University, 4700 Keele Street, Toronto, M3J 1P3 Canada.
[2]Department of Earth and Space Science and Engineering, York University, 4700 Keele Street, Toronto, M3J 1P3 Canada.

Received 26 November, 2015; Accepted 22 March, 2016

Two models for raindrop growth in clouds are developed and compared with an interpretation to elucidate the rain drop relationship among both the models. A continuous accretion model is solved numerically for drop growth from 20 to 50 microns, using a polynomial approximation to the collection kernel, and is shown to underestimate growth rates. A Monte Carlo simulation for stochastic growth have also been implemented to demonstrate the discrete drop growth. The approach models the effect of decreased average time between captures as the drop size increases. It is found that the stochastic model yields a more realistic growth rate, especially for larger drop sizes. It is concluded that the stochastic model shows faster droplet accumulation and hence shorter time for drop growth.

Key words: Raindrop growth, continuous collection, stochastic collection, Monte Carlo method, implicit and semi-implicit technique.

INTRODUCTION

In clouds, the development of a size distribution of rain drops with radius R, as they collect droplets of radius r, is described by a nonlinear differential equation relating the mean number concentration of droplets $N(r)$ to the rate at which drops and droplets collide and coalesce. The effect of mixing between upwards and downwards moving entities is to reduce the concentration of droplets in the ascending air. The super supersaturated created in the updraft is then distributed over fewer drops, permitting them to grow to larger sizes. The saturated cannot persist and much less grow unless the environment is super-saturated (H >100%) by the amount equal to the vapor pressure of the droplet by according to Richard et al. (1992).

Rain drop collision does not guarantee coalescence. When a pair of drops collides they may subsequently: (i) bounce apart, (ii) coalesce and remain so, (iii) coalesce temporarily but then break apart, retaining their initial identities, (iv) coalescence temporarily but then break apart to a number of smaller drops. For sizes smaller than 100 microns in radius, the important interactions are (i) and (ii), described by Barnet (2011) and Rogers and Yau (1989).

In stochastic raindrop growth, coalescence can broaden the droplet spectrum, but is hindered in the early growth stages by the fact that the collection efficiencies between

*Corresponding author. E-mail: E-mail: rehanrul@yorku.ca.

small droplets are extremely small. Coalescence is not sufficient to account for rain development over short periods as shown by an earlier study (Robertson, 1974). It is now recognized that statistical effects are crucial in the early stages of coalescence. Consequently a stochastic coalescence model provides a convenient means to describe this process (Kostinski and Shaw, 2005a, b). It is also found that the positions of droplets in a natural cloud were not perfectly random but there was some degree of correlations with local fluctuations in droplet number density as explained by Uchida and Ohta (1969, 1971). According to Rogers and Yau (1989), as droplets grow, their collection efficiencies increase, increasing the probability of coalescence. Once it begins coalescence proceeds rapidly, as indicated by the fast decline in the number of drops. At the same time, super saturation increases sharply because the drops, now fewer in number, are no longer able to consume the excess vapor at the rate it is created. But overall in nature, the effect on coalescence of charge on the drops, comparable to that observed on raindrops in nature is small according to Kenrick and Walter (1951).

In general, the continuous and stochastic growth of rain drop are classified by the relative amount of water collected from the different sizes of small droplets to large droplets, which is mainly dependent upon the mass and size of the droplets. Droplets growing according to the continuous model collect most of their water by capture of droplets while droplets growing by stochastic model collect water from droplets of all the small sizes. According to Berry (1967), the average rate of mass and size increase of n^{th} droplet due to the capture of r^{th} droplets is equal to the product of the collection kernel (volume swept out per unit time and the mass density function (mass per unit volume per unit size of interval).

The effects of turbulence in a cloud can be modeled by a probabilistic collection kernel where the magnitude of the collection kernel indicates, the importance of turbulence (Berry, 1967). Turbulence is very important and creates a positive correlation between super-saturation and droplet surface area fluctuation that increases as the turbulent scale separation explained by Gaetano et al. (2015).

In this work we developed and compared two models for raindrop growth in clouds based on continuous accretion and stochastic technique by using numerical solution and Monte Carlo simulation. It is found that the stochastic model yields a more realistic growth rate, especially for larger drop sizes. We applied MATLAB/MAPLE13 for numerical techniques and programming. This article basically reviews the growth of rain drop and compared their trends of growth by continuous and stochastic techniques in clouds (for example, Rogers and Yau, 1989; Pruppacher and Klett, 1997).

METHODOLOGY

Consider a collector (larger) drop of radius R that is falling relative to a field of smaller droplets of radius r. The rate at which the collector collides with the smaller droplets is proportional to the shared *collision volume*, $V_c(R,r)$, which is given by the cross-sectional areas of both the drop and the droplet and their vertical velocities $u(R)$, $u(r)$. Derivation and discussion of Equations can be found in Long (1973); Long and Manton, (1974) and Robertson (1974).

$$V_c(R,r) = \pi(R+r)^2\{u(R)-u(r)\} \tag{1}$$

The probability that a collision between a drop and a droplet results in an actual capture (coalescence) is described by the collection efficiency *E(R,r)*. Given that the mean number of droplets within the collision volume is $V_c(R,r)N(r)$, where *N(r)* is the mean number concentration of droplets, the probability per unit time that a drop captures a droplet is:

$$\begin{aligned} P(R,r) &= V_c(R,r)N(r)E(R,r) \\ &= \pi(R+r)^2\{u(R)-u(r)\}N(r)E(R,r) \end{aligned} \tag{2}$$

The realistic growth of a collector drop is discrete, where capture of each droplet increases the mass of the drop $M(R)$ by the finite droplet mass $m(r)$. The collector drop also grows stochastically, where each capture has a probability between 0 and 1. The mean growth rate of the collector drop is described by:

$$\frac{dM(R)}{dt} = m(r)P(R,r) \tag{3}$$

As a first approximation, we consider the simplest type of model for collection growth, the continuous model, as:

$$\frac{dM(R)}{dt} = m(r)\pi(R+r)^2\{u(R)-u(r)\}N(r)E(R,r) \tag{4}$$

$$\frac{dM(R)}{dt} = K(R,r)w_L(r) \tag{5}$$

Here we have two factors: the droplet collection kernel $K(R,r) = \pi(R+r)^2\{u(R)-u(r)\}E(R,r)$, and the liquid water content of the droplets, $w_L(r) = m(r)N(r)$. A method for deriving an analytical solution for the droplet collection equation, using a polynomial approximation to the kernel, $K_P(R,r) = cx^2$. Here c is a scaling factor and $x \equiv V(R)$ is the collector drop volume. Then the collection equation becomes:

$$\begin{aligned} \frac{dM(R)}{dt} &= cV^2 m(r)N(r) \\ \frac{dV(R)}{dt} &= cV^2 v(r)N(r) \end{aligned} \tag{6}$$

Here, *v(r)* is the droplet volume. An analytical solution for *V(t)* is found by integrating the above equation, to give:

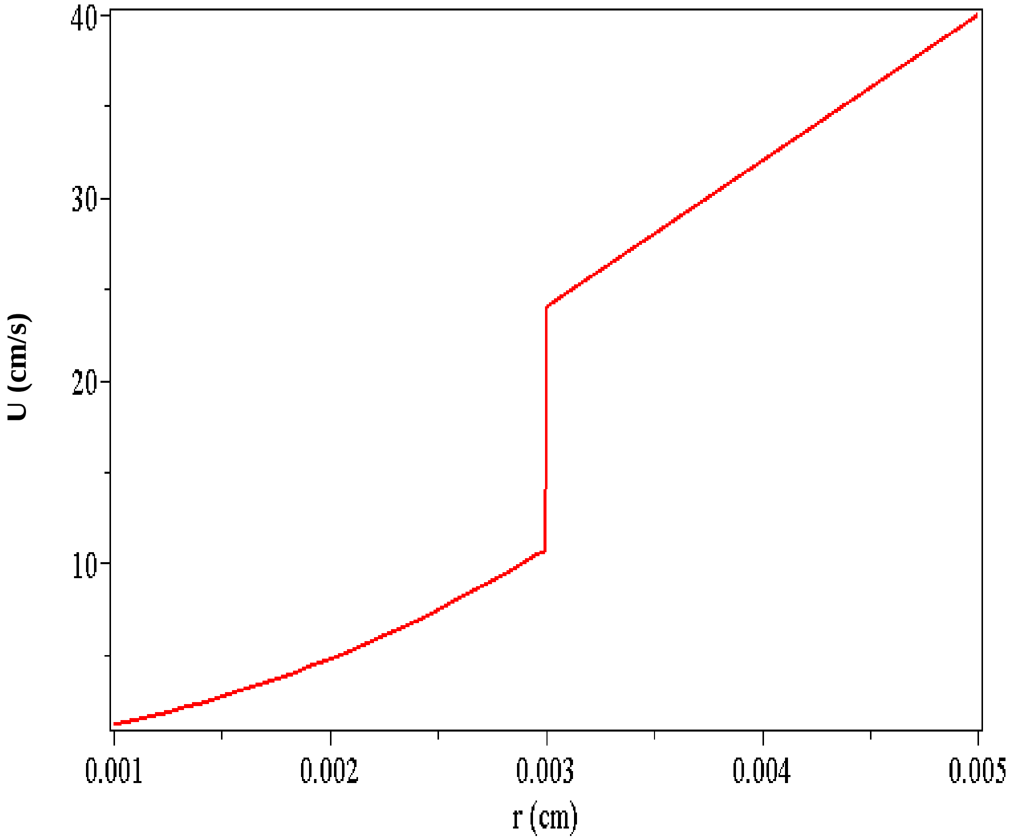

Figure 1. Droplet terminal velocity as a function of droplet size.

$$V(t)=\frac{1}{(1/V_0-cNvt)} \tag{7}$$

and V_o is the initial collector drop volume and c = 1.1 x 10^{10} $cm^{-3}s^{-1}$ is the constant related to the polynomial kernel according to Long and Manton (1974). For the continuous model of collection growth, equation (8) is numerically solved using an implicit or semi-implicit integration scheme. The implicit scheme is:

$$\frac{(V_{n+1}-V_n)}{\Delta t}=cv(r)N(r).V_{n+1}^2 \tag{8}$$

The semi-implicit equation is:

$$\frac{(V_{n+1}-V_n)}{\Delta t}=cv(r)N(r).V_{n+1}V_n \tag{9}$$

A Monte Carlo simulation of stochastic drop growth have also been implemented. First, we have calculated the time interval Δt to perform a discrete simulation step for which the probability of capture $q=P(R,r)\Delta t$, where q is chosen to be a small value such as 0.1 as suggested by Long (1973). If a uniformly distributed random number x between 0 and 1 is generated and $x > q$, then no capture occurs during the time interval $\Delta t = q/P(R,r)$. If $x \le q$, a capture is deemed to have occurred and $M(R)$ is increased by m(r). Before the next time step, $P(R,r)$ and Δt have been recalculated by using the proposed model which corresponds to the value of R according to Robertson (1974).

Droplet terminal velocity

One important factor in drop formation is the droplet terminal velocity. In general, when downward net gravitational force is equal to upward drag force (that is, $F_G = F_{drag}$), the droplet reaches a steady fall speed, its terminal velocity. Terminal velocities depend mainly on the size of the droplet. Figure 1 shows the droplet terminal velocity as a function of its radius, with different droplet regimes showing different behaviors agreed by the results of Rinehart (1990). By Rogers and Yau (1989), for small droplet sizes ($r \le 30\mu m$), flow is completely dominated by air viscosity, and the terminal velocity increases quadratically: $u = k_1r^2$ with $k_1 = 1.19 \times 10^8\ s^{-1}m^{-1}$. For larger sizes (30µm ≤ r ≤ 10^3µm), flow is turbulent and is assumed to be homogeneous and isotropic, and the velocity grows linearly: u = k_3r with $k_3 = 8 \times 10^3\ s^{-1}$.

Collection efficiency

The probability that a collision between a drop of radius R and a

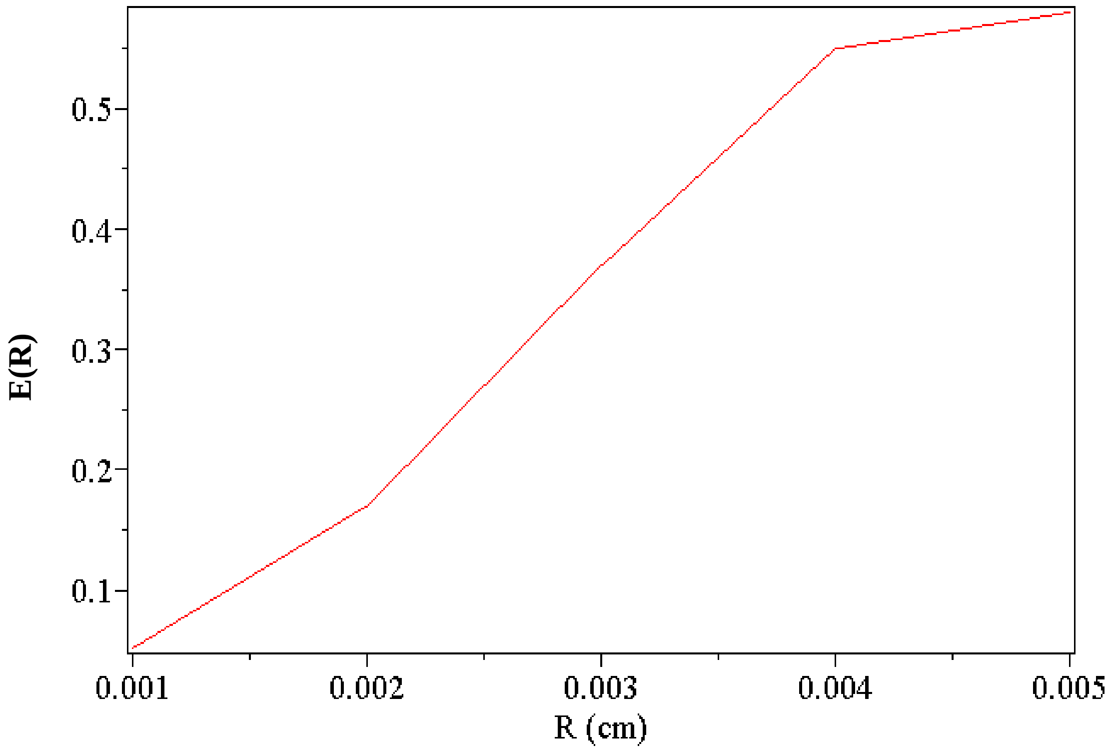

Figure 2. Collection efficiency as a function of drop radius R, for collisions with droplets of radius r = 10 µm.

droplet results in a capture is called efficiency and is given by $E(R,r) = x_o^2/(R + r)^2$. The value of R is important for any size of collector drop and E is small for small values of r/R. The collision efficiency as a function of drop radius R increases with drop size, as shown in Figure 2.

Accuracy and sensitivity of the models

The accuracy, sensitivity and complete statistical analysis of both the models have been done by Monte Carlo trials with q=0.1, N=1000, capture probability and average growth-times T_{avg} (q) computed for 100 values of q in the range [0.01, 1.0] as shown in Figure 4 to 6, respectively.

RESULTS AND DISCUSSION

Drop growth have been computed for an initial collector drop radius of $R_i = 20$ µm and continued until the drop reached a final radius $R_f = 50$ µm. The collected droplets have a radius of $r = 10$ µm and a concentration $N(r)$ = 100 cm^{-3}. For continuous growth both numerical techniques have been applied and the results are plotted in Figure 3 along with the analytical solution. The stochastic growth was computed using a capture probability of q=0.1. The average growth time by using Monte Carlo runs is also shown in Figure 3. The analytical solution have been shown as a thick red line, with semi-implicit and implicit numerical solutions shown as circles and squares, respectively. The average growth time computed with the stochastic model have been plotted as a thick dashed-dot line, with the two standard deviation range bounded by the dotted lines and shaded in yellow. While the average result shows the continuous growth curves are in close agreement, it is evident that the drop growth rate becomes slower than the Monte Carlo solution as the drop radius increases.

In the Monte Carlo technique, the average time between captures gets smaller as the drop grows. As expected, after a sufficiently large number of captures i.e. at a larger drop radius R, the growth curves stabilize, and increase in parallel to the continuous growth curve also explained by Robertson (1974). The various Monte Carlo runs exhibit statistical variations, but yield shorter average growth time than the continuous model, since their rates increase substantially once the collector drop radius exceeds about 25 microns. The 25 microns were also reported as barrier to stochastic growth rate of rain by Hawkes (1972).

Model sensitivity

To explore the statistical behavior and accuracy of the discrete model, a large number (N=1000) of Monte Carlo

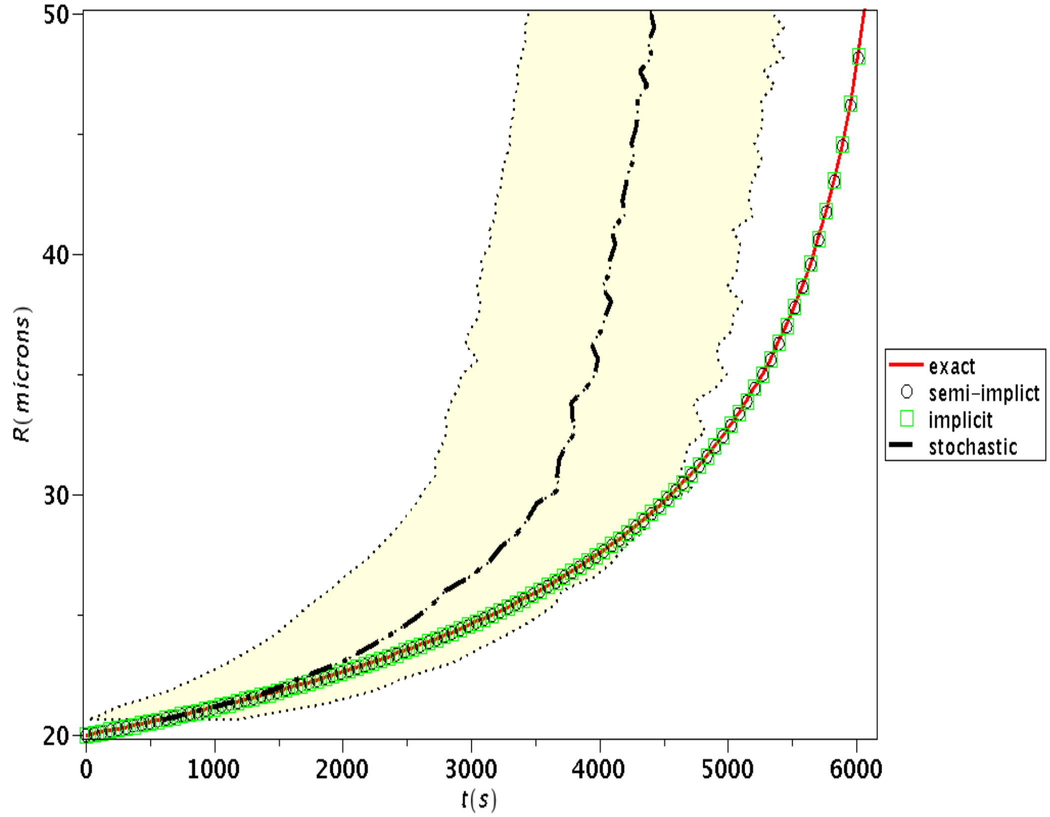

Figure 3. Collector drop radius R as a function of time for continuous and stochastic growth models.

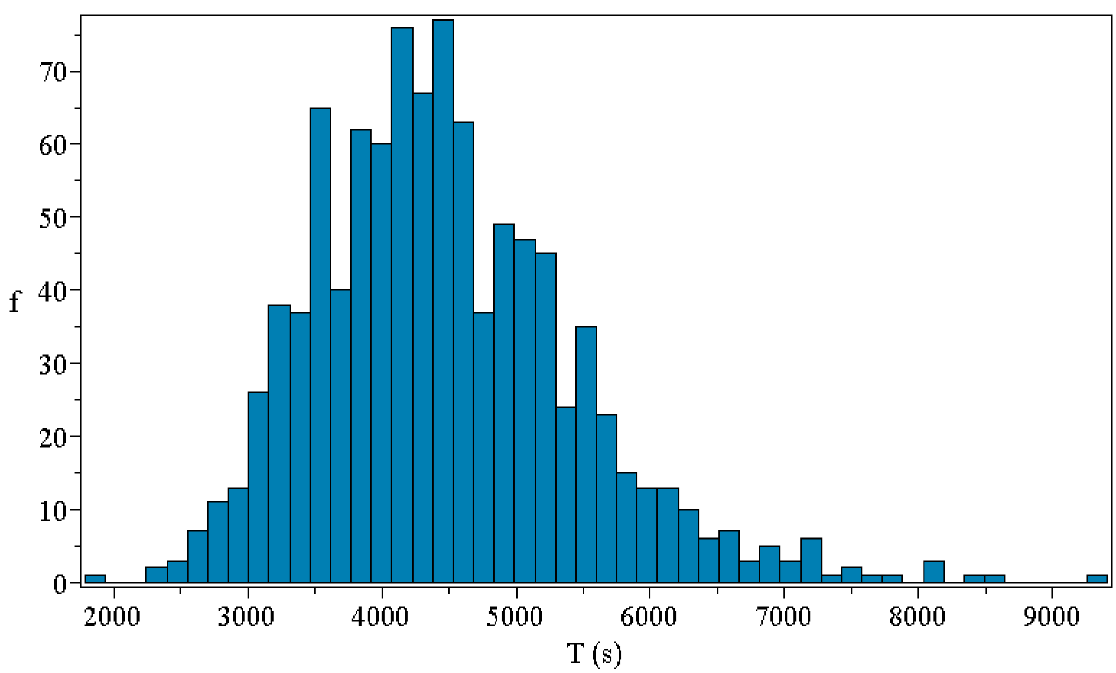

Figure 4. Distribution of collector drop growth times T, obtained from N=1000 Monte Carlo trials with q=0.1: T_{avg} = 4445 s, σ = 953 s.

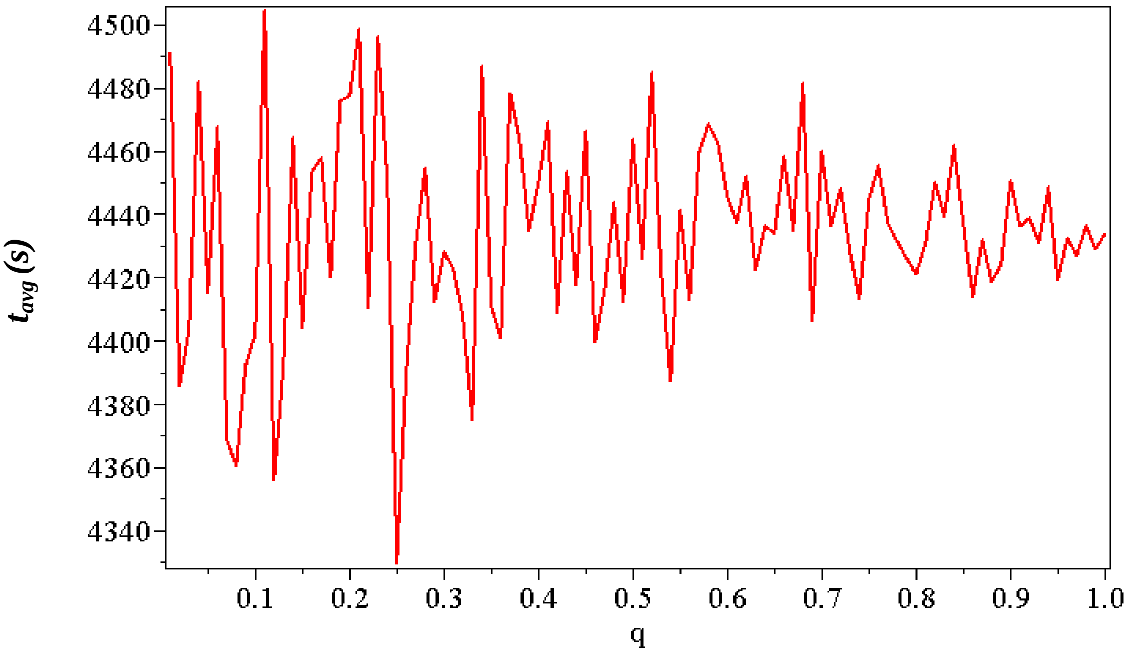

Figure 5. Average growth times obtained using 100 equally-spaced values of q in the range from 0.01 to 1.0.

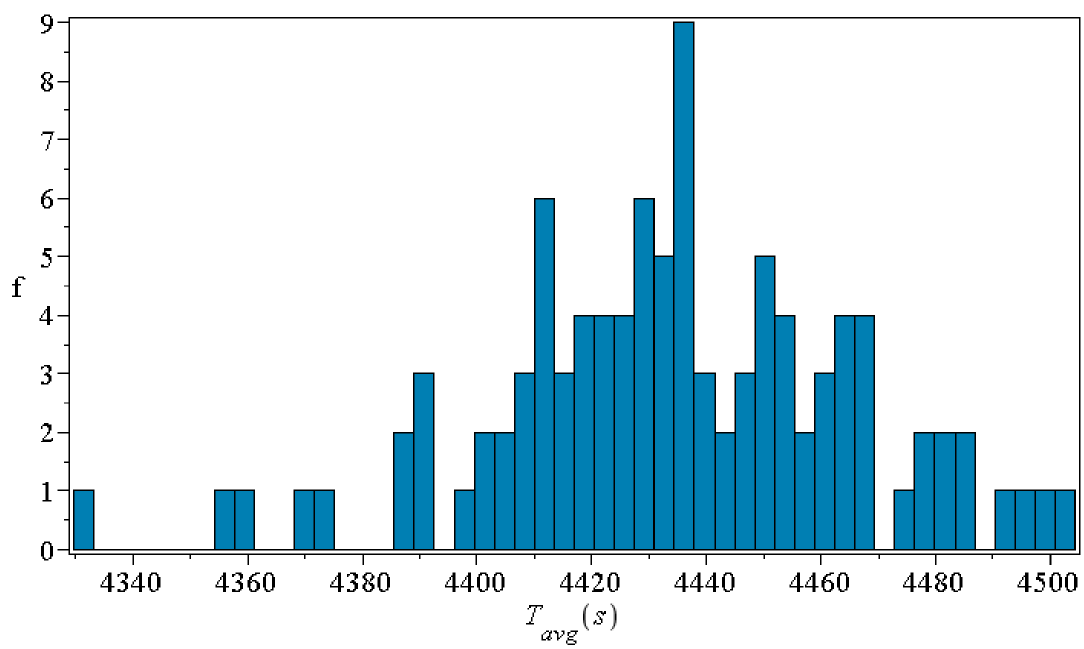

Figure 6. Distribution of average growth times obtained using 100 equally-spaced values of q in the range from 0.01 to 1.0: $< T_{avg} >$ = 4434 s, σ = 32 s.

runs have been performed, yielding a distribution of drop growth times, shown in Figure 4. This distribution has a mean growth time, T_{avg} = 4445 s, with a standard deviation σ = 953 s (a 22% uncertainty). To check the sensitivity of the model to the capture probability, average growth-times T_{avg} (q) have been computed for 100 values of q in the range [0.01, 1.0]. The resulting values are shown in Figure 5 and their distribution are shown in Figure 6, with a mean < T_{avg} > = 4434 s and σ = 32 s. This demonstrates the low sensitivity of the model to variation of q, with only 0.7% variation in the average growth time.

Conclusion

Continuous and stochastic models have been used to simulate the accretion growth of an individual collector drop from a starting size of 20 microns to a final size of 50 microns. In the continuous accretion case, the time for drop growth is unrealistically long due to large accumulation of water contents. In contrast, the stochastic model showed faster droplet accumulation and hence shorter times for drop growth. For a fixed choice of capture probability q=0.1, the average growth time T_{avg} has an uncertainty of 22%. However the sensitivity of T_{avg} to the capture probability was found to be small: when q is varied between 0.01 and 1.0, it showed only a 0.7% variation. Finally, it is concluded that all the water mass moves with the mode in the stochastic model, whereas in the continuous model, most of the water mass must remain on the small droplets. This work leads to a significant role for the analysis of any future rain drop development methodology and any theoretical numerical weather forecasting test.

Conflict of Interests

The authors have not declared any conflict of interests.

ACKNOWLEDGEMENTS

This work is supported by Physics & Astronomy and Earth and Space Science Department of York University, Toronto, Canada. The author's also wishes to the members of Thoth Technology Inc. for their kind technical support concerning various aspects of the material presented here.

REFERENCES

Barnet P (2011). Rain drop growth by collision and coalescence. University of reading. Sch. Math. Phys. Sci. pp. 1-52.

Berry EX (1967). Cloud Droplet Growth by Collection. J. Atmos. Sci. 24: 688-701.

Gaetano S, Francesco P, Luca B, Rodrigo C (2015). Continuous Growth of Droplet Size Variance due to Condensation in Turbulent Clouds. Phys. Rev. Lett. 115(184501):1-5.

Hawkes RL (1972). The 15–25 µm barrier to drop growth in warm rain. Atmosphere 13(2):62-76.

Kenrick G, Walter H (1951). A Laboratory Investigation of the coalescence between large and small water drops. J. Meteor. 8:7-16.

Kostinski AB, Shaw RA (2005a). Fluctuations and Luck in Droplet Growth by Coalescence. Bull. Amer. Meteorol. Soc. 86:235-244.

Kostinski AB, Shaw RA (2005b). Supplement obtaining the drop size distribution. Amer. Meteorol. Soc. BAMS:ES1-ES2.

Long AB (1973). Solutions to the Droplet Collection Equation for Polynomial Kernels. J. Atmos. Sci. 31:1040-1052.

Long AB, Manton MJ (1974). On the Evaluation of the Collection Kernel for the Coalescence of Water Droplets. J. Atmos. Sci. 31:1053-1057.

Pruppacher HR, Klett JD (1997). Microphysics of Clouds and Precipitation. Second Revised and Enlarged Edition with an Introduction to Cloud Chemistry and Cloud Electricity, Kluwer Academic Publishers. Dordrecht. 954 p.

Richard J, Doviak D, Zmic S (1992). Doppler Radar and Weather Observations. 2nd Edition. Academic Press. ISBN-0-12-221422-6. 211 p.

Rinehart RE (1990). Radar for Meteorologists. University of North Dakota. Office of the President. 218 p.

Robertson D (1974). Monte Carlo Simulations of Drop Growth by Accretion. J. Atmos. Sci. 31:1344-1350.

Rogers RR, Yau MK (1989). A Short Course in Cloud Physics. Pergamon Press 290 p.

Uchida E, Ohta S (1969). A Simulation approach to the formation of precipitation particles using the Monte Carlo method. J. Meteor. Soc. Japan. 47:279-291.

Uchida E, Ohta S (1971). Simulation approach to the formation of precipitation particles by aid of the Monte Carlo method. Proc. Inter. Cloud Physics. Conf. London Roy. Meteor. Soc. pp. 127-131.

academicJournals

Vol. 8(3), pp. 39-51, April 2016
DOI: 10.5897/IJWREE2016.0636
Article Number: 84D7FB158331
ISSN 2141-6613

http://www.academicjournals.org/IJWREE

International Journal of Water Resources and Environmental Engineering

Full Length Research Paper

Spatial and temporal variability of dry spell lengths and indication of climate change in rainfall extremes at Tekeze River Basin, Ethiopia

Michale Gebrekiros Gebreselassie[1]* and Semu Ayalew Moges[2]

[1]Department of Water Resources and Irrigation Engineering, Aksum University, Ethiopia.
[2]Chair, Climate, Hydrology and Water Resources Systems (CHWRS), Addis Ababa University, Ethiopia.

Received 20 January, 2016; Accepted 22 March, 2016

Understanding weather extremes and climate variability both in space and time based on historical surface observed climate data at watershed is very crucial as it is used as in put for applying the seasonal forecast given by National Hydrological and Meteorological Agencies, in decision making in agricultural activities, water resources projects, rainfall-runoff modeling, and for drought risk identification and assessment. This study examined the spatio-temporal variability of dry spell length in Kiremt (June to September) season and trend detection, as a means of indication for climate change, in rainfall extremes over Tekeze river basin, Ethiopia. Daily rainfall indices were used over the basin based on data available from 24 meteorological stations having variable record length spanning from 1960-2009 with available data from 1992-2009 for most of the stations. Data quality control was done for infilling missing values and main quality tests of outliers and homogeneity tests. Temporal variability was analyzed by coefficient of variability and temporal trends were analyzed using Mann-Kendall method. Spatial distribution and variability was investigated using ordinary kirging interpolation technique. The results showed that: (1) The dry spell lengths for the months of kiremt season showed high temporal variability; (2) The dry spell lengths in the months of Kiremt season were shown to be higher in north-east and north-west of the river basin than the other parts; (3) The dry spell lengths were higher in the months of June and September and changed more rapidly in the basin than dry spell lengths in July and August; and (4) A significantly increasing trend on the 95th percentile of daily rainfall was found at Gonder meteorological station and significantly decreasing trend on the 90th percentiles of daily rainfall was found at Mekelle meteorological station.

Key words: Dry spell lengths, extreme rainfall, climate change, spatial variability.

INTRODUCTION

The use of implementing expensive and elaborate rainfall monitoring networks at a basin is to capture and understand the spatial and temporal variability of rainfall. Rainfall is the most important hydrological variable and it varies considerably over space and time. This variability makes it a major source of risk for agricultural production

*Corresponding author. E-mail: mgk169@gmail.com. Tel: +251-0931808915.

especially for a country like Ethiopia whose economy is dependent on rain-fed agriculture. This sector is highly sensitive to the spatial and temporal variability of rainfall and much below normal rainfall years in the country resulted in low agricultural production and as a consequence it affected millions of people in the country (Wolde-Mariam, 1984; Degefu, 1987; Hurni, 1993; Camberlin, 1997; Aredo and Seleshi, 2003). The spatial and temporal variability of water resources is also affected due to rainfall variability. Rainfall variability has greater impact on hydrology and water resources (Novotny and Stefan, 2007). The study of rainfall variability in time and space over long period of time is basic for water resources management and decision making strategies. According to Michaelides et al. (2009) understanding rainfall variability in time and space helps greatly for agricultural planning, rainfall-runoff modeling, water resources assessments and climate change and environmental impact assessments.

Even though rainfall monitoring networks are sparsely distributed at the country, many researches have been conducted to understand rainfall variability using the existing stations in the country. The previous researches on the rainfall variability have been done on different spatial and temporal scales. Examples: Osman and Sauerborn (2002) studied the rainfall variability of the central highlands of Ethiopia for the main rain season (June to September) using 11 stations of data from (1898-1997) and noted a decreasing trend of seasonal rainfall in their study. Seleshi and Zanke (2004) studied the rainfall variability of Ethiopia at seasonal and annual time scales using 11 stations with data from (1965-2002) and noted no trend of rainfall at annual and seasonal time scales for Central, Northern and Northwestern Ethiopia highlands. But with significant trend over Eastern, Southern and Southwestern Ethiopia. Cheung et al. (2008) studied the rainfall variability of 13 watersheds of the whole Ethiopia using 134 stations of data between 1960 and 2002 at annual and seasonal time scales. For Tekeze river catchment they utilized nine rainfall stations and found no trend in the rainfall time series. The above previous studies, with contradicting conclusions, did not studied the rainfall variability at daily time and spatial scales and used few number of stations compared to their area of studies.

This study examined the variability dry spell lengths and trend detection in rainfall extremes at the Tekeze river basin both in time and space. It tried to answer such questions: (i) to what extent do the dry spell lengths vary in time and space? (ii) Which part of the river basin is more affected by dry spell lengths? (iii) How do the dry spell lengths vary from location to location in the river basin? And (iv) is there any climate change indication in rainfall extremes in the basin?

Description of the study area

Tekeze basin is one of the major river basins of Ethiopia. The basin is located in the Northern western part of Ethiopia (Figure 1). The basin consists of the main catchments of Tekeze, Angerb and Goang rivers. This study focuses only on the Tekeze river basin. Tekeze river basin is located at $11^{0}40'12.20''$ N to $14^{0}45'42.29''$ N and $36^{0}32'07.70''$ E to $39^{0}46'23.89''$E in the Northern western part of Ethiopia. The Tekeze river basin has an area of 63,109.1 km^2 with its out let located at 14.259^{0}N and 36.560^{0}E. The river basin has a minimum elevation of 537 m.a.s.l and a maximum elevation of 4517 m.a.s.l. The annual rainfall variability in the Tekeze basin is very high. The mean annual rainfall in the basin ranges from about 600 mm in the north east to over 1200 mm in the high lands of south west (Belete, 2007). Generally the rainfall in the basin is high affected by local factors like topography and micro-climate in the basin (Amare, 1996). The year-to- year variability of annual rainfall totals in the basin is very high showing coefficient of variability ranging from 0.2 in the high lands of the basin to 0.4 over its low land part (Belete, 2007). The mean are temperature in the basin varies from about 10°C in the highlands of the basin to over 26°C on its lowlands.

METHODOLOGY

In order to examine the spatial and temporal variability of rainfall in the Tekeze river basin, the study approach is summarized as follows and details are presented in the subsections below. A Digital Elevation Model (DEM), which is 90 m spatial resolution, of the Tekeze river basin is downloaded from the website of http://srtm.sci.cgiar.org/SELECTION/input /input Coord.asp. And the location of each meteorological station was obtained from the website of www.nma.org.et of the National Meteorological Agency of Ethiopia. After delineating the Tekeze river basin from the DEM and identifying the meteorological stations which could represent the basin, quality control for the daily data of each station have been done. Assessment for quality of the data of each station was done by filling missing data, testing for outliers and testing for temporal homogeneity. After checking for outlier and making adjustment and identifying only stations with homogeneous rainfall data, rainfall indices were derived and the temporal and spatial variability of the indices over the basin were done.

Data collection

In this study, daily rainfall data of the Tekeze river basin for the period from 1960-2009 with available data from 1992-2009 for most of the stations were obtained from the archives of the National Meteorological Agency (NMA) of Ethiopia. The dataset contains 24 meteorological stations. The spatial distribution of those meteorological stations is shown in Figure 2. And Table 1 illustrates a generalized geographic location, period of recorded rainfall, and percent of missing values information of each selected stations used for this study.

Data quality and control

Infilling missing daily rainfall

Infilling missing daily rainfall data with percent of missing at most 10

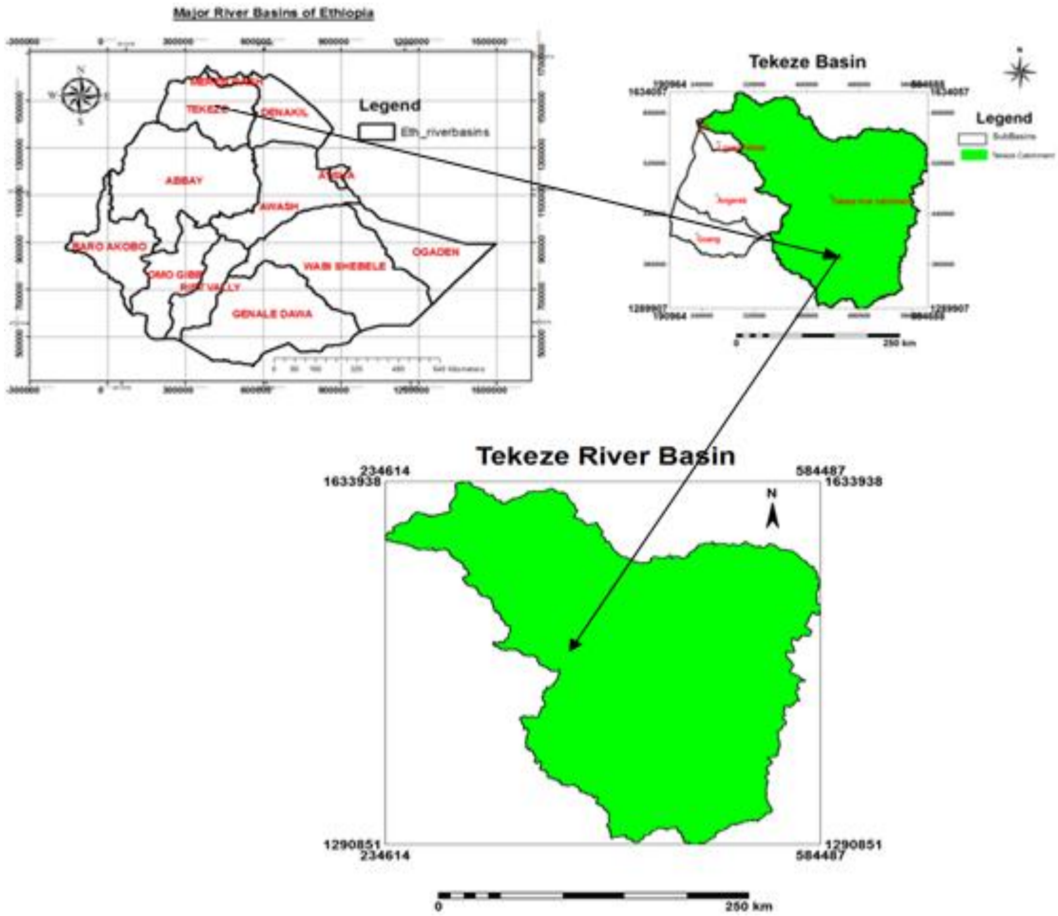

Figure 1. Shows the major river basin of Ethiopia, the Tekeze basin and the Tekeze River basin.

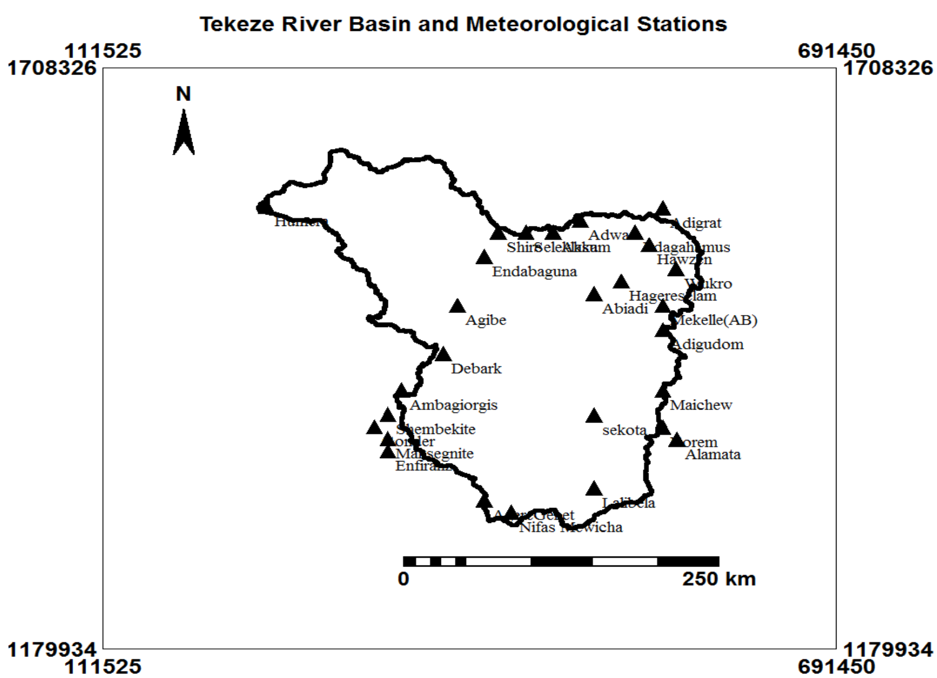

Figure 2. Spatial distribution meteorological stations over Tekeze river basin.

Table 1. Geographical location, period of recorded rainfall and percent of missing values.

ID	Station Name	Longitude	Latitude	Altitude	Start year	End year	Available year	% of Miss
1	Adigudom	39.5	13.3	2090	1992	2007	16	4
2	Adigrat	39.5	14.3	2485	1992	2007	16	3
3	Adwa	38.9	14.2	1913	1992	2007	16	2
4	Aksum	38.7	14.1	2101	1992	2007	16	3
5	Edagahamus	39.3	14.1	1972	1973	2007	35	10
6	Hawzen	39.4	14	2253	1992	2009	18	3
7	Humera	36.6	14.3	587	1980	2009	18	10
8	Korem	39.5	12.5	2454	1992	2009	18	2
9	Maichew	39.5	12.8	2475	1992	2009	18	2
10	Mekelle(AB)	39.5	13.5	2252	1960	2009	50	8
11	Seleklaka	38.5	14.1	2014	1995	2009	15	5
12	Shire	38.3	14.1	1901	1992	2009	18	1
13	Wukro	39.6	13.8	2077	1992	2009	18	10
14	Ambagiorgis	37.6	12.8	2942	1992	2009	18	7
15	AgereGenet	38.2	11.9	2447	1992	2007	16	10
16	Enfiranz	37.5	12.3	1832	1992	2007	16	10
17	Gonder	37.4	12.5	2033	1960	2008	49	7
18	Shembekite	37.5	12.6	2301	1992	2008	17	4
19	Debark	37.9	13.1	2807	1992	2009	18	7
20	Lalibela	39	12	2500	1992	2007	16	9
21	Nifas Mewicha	38.4	11.8	2947	1992	2007	16	9
22	Agibe	38	13.5	1128	1998	2007	10	3
23	sekota	39	12.6	2275	1997	2006	10	7
24	Abiadi	39	13.6	1647	1998	2007	10	5

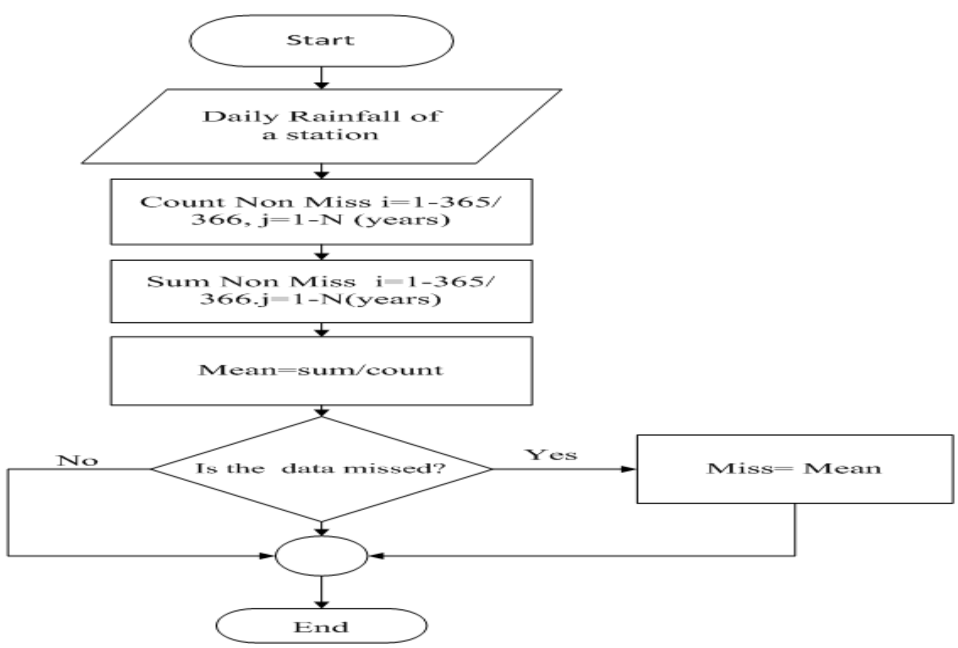

Figure 3. Flow chart showing infilling daily rainfall data by long-term mean.

of the recorded data can be done by sample mean taking in to account the correlation between the daily rainfalls is negligible (Presti et al., 2010). Therefore, all the stations having daily missing rainfall data at most 10% are filled by mean of each day. Figure 3

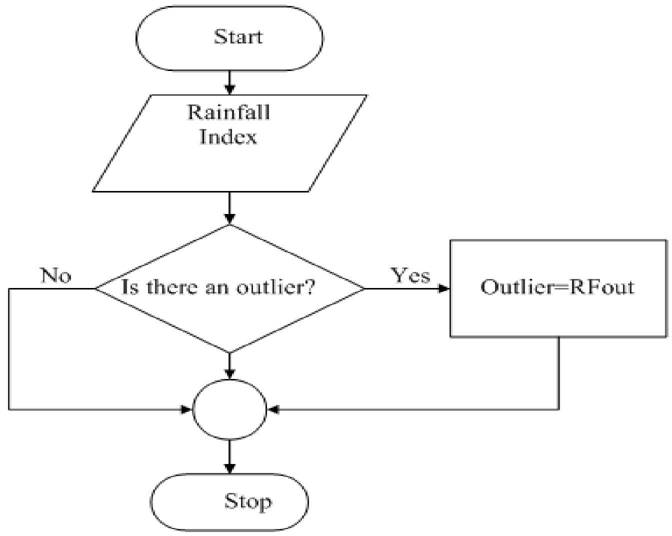

Figure 4. Flow chart showing how to adjust outliers.

shows how to fill the missing daily rainfall of each station.

Outlier detection and adjustment

The identification of outliers has been the primary emphasis of quality control work (Gonzalez-Rouca et al., 2001; Göktürk et al., 2008). Outliers are values greater than a threshold value specific for each time series, defined by

$RF_{out}= RF_{0.75} +3*IQR$

Where RF_{out} is a threshold value, $RF_{0.75}$ is the third quartile and IQR is the inter quartile range and any outlier can be replaced by its threshold value as stated by Gonzalez-Rouca et al. (2001) and Göktürk et al. (2008). In order to keep the information of extreme values in the data, outliers can be replaced by the thresh hold value in the data. For keeping the outliers of each rainfall indices of each station, a threshold value was calculated and any outlier in each index could be replaced by the threshold value (RFout). Flow char how to adjust outlier is shown in Figure 4.

Homogeneity test

A rainfall time sequence is called homogeneous when its variability is as the result of weather and climate (Conrad and Pollak, 1950). Long period recorded rainfall can be non homogeneous when affected by non-climatic factors that make them unrepresentative of the actual climatic variations occurring over the time (Peterson et al., 1998). Non homogeneity of the time sequence can be occurred due to change in location of the rainfall station, instruments, formula used to calculate the statistical parameters, observing practices and station environments (Göktürk et al., 2008). In order to be sure that daily rainfall recorded by all the stations in this study are representative in their areas of location and their variability is only due to climatic and weather process not other factors, three homogeneity test methods were used the Pettitt's test (Pettitt, 1979), the Standard Normal Homogeneity Test (SNHT) (Alexandersson, 1986), and the Buishand's test (Buishand, 1982). The homogeneity tests by the three methods were done on daily maximum rainfall (MaxRF), daily mean rainfall (MEANRF) and annual rainfall (ANNUALRF) of each station. The explanations of the three methods of homogeneity test are shown in Figure 5.

Derivation of rainfall indices from daily rainfall data

Six rainfall indices describing different aspects of rainfall regime were derived from the daily rainfall in this study. The indices have been used in various parts of Africa. Many authors define a dry spell as n consecutive days without appreciable rainfall (Stern, 1980; Sivakumar, 1992; Sharma, 1996; Ceballos et al., 2004; Gong et al., 2005). In many studies, days with rainfall less than 0.1 mm per day are considered a dry spell. Mean values of each index were calculated at annual time scale and seasonal time scales (June to September). Table 2 provides the name of each index with its explanation.

Rainfall indices temporal variability and trend detection

The coefficient of variation (CV) is used as statistical descriptor of the rainfall indices temporal variability of the stations over Tekeze basin. The CV of a variable is the standard deviation the variable divided by its mean. High CV of a variable indicates high temporal variability of the variable. The existence of a trend of a time series of the rainfall indices can be quantified by least squares regression in stations having at least 30 year of recorded data and the trend statistical significance can be test by Mann-Kendall (MK) test which is used in this study. The rainfall indices at Gonder, Mekelle and Edagahamus meteorological stations having daily rainfall of period 1960-2008, 1960-2009 and 1973-2007 respectively were subjected to non-parametric Mann-Kendall test to detect trend as means of indication for climate change.

Rainfall indices spatial distribution and variability

In order to examine the spatial distribution and variability of the rainfall indices from the meteorological stations, it was necessary to estimate the point rainfall index at unrecorded locations from the values at the surrounding stations. Kirging interpolation technique was used in this paper. This method is increasingly preferred

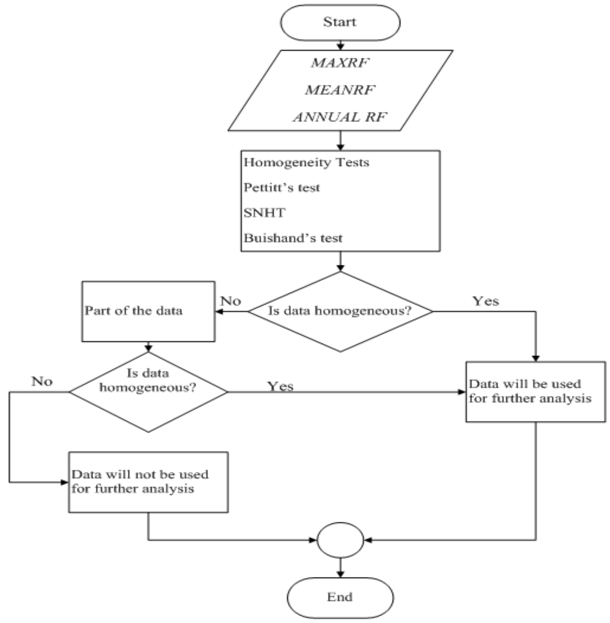

Figure 5. Flow chart of non homogeneity tests.

Table 2. Name of the six selected indices with their explanations.

S/N	Explanation	Index Name
1	Dry day	A day with rainfall of< 0.1mm in a day in a year
2	Dry spell length for June	Two or more consecutive dry spells in June
3	Dry spell length for July	Two or more consecutive dry spells in July
4	Dry spell length for August	Two or more consecutive dry spells in August
5	Dry spell length for September	Two or more consecutive dry spells in September
6	90^{th} percentile	The 90^{th} percentile of daily rainfall in a year
7	95^{th} percentile	The 95^{th} percentile of daily rainfall in a year

because it capitalize on the spatial correlation between neighboring observations to predict attributed values at un sampled locations (Goovaerts, 1999). It is not simply based on an estimation of the unknown value as a function of the distance. In addition to that it implements the function of unknown spatial autocorrelation between the values of the sample points. In addition, (Tabios and Salas, 1985) have shown that geostatistical prediction techniques (kriging) provide better estimates of rainfall than conventional (Thiessen Polygon and Inverse Distance Weighted (IDW) methods. Of the types of kirging, especially ordinary kirging was used in this study by using the Integrated Land and Water Information System (ILWIS) which is an integrated Geographical Information System (GIS) and Remote Sensing software. The best fitting models (Exponential, Spherical and Circular) are identified by adjusting the nugget, range and sill parameters from the experimental semi-variogram of the chosen model by visual inspection. Model variogram is used to develop interpolated surface to predict spatial continuity in the river basin by ordinary kirging. The limiting distance that is the maximum search radius to find stations which will be taken in to account during the interpolation of the indices is determined by doing pattern analysis of the stations with reference to the area of the basin. The spatial variability of all the indices can be analyzed using ordinary kirging interpolation technique. In Ordinary Kriging the randomized spatial function is non-stationary and the mean varies over the area of interest. Ordinary Kriging amounts to re-estimating the mean at each new location. In Ordinary Kriging, you can influence the number of points that should be taken into account in the calculation of an output pixel value by specifying a limiting distance and a minimum and maximum number of points. Only the points that fall within the limiting distance to an output pixel will be used in the calculation for that output pixel value. Ordinary Kirging needs three steps Spatial Correlation, Empirical Semi-Variogram and modeling semi-variogram as shown in the flow chart Figure 6.

RESULTS AND DISCUSSION

Temporal variability of dry spell lengths for June, July, August and September (months of the kiremt season) over Tekeze river basin

There is very high year-to-year variability of dry spell lengths for the months of Kiremt season (June, July,

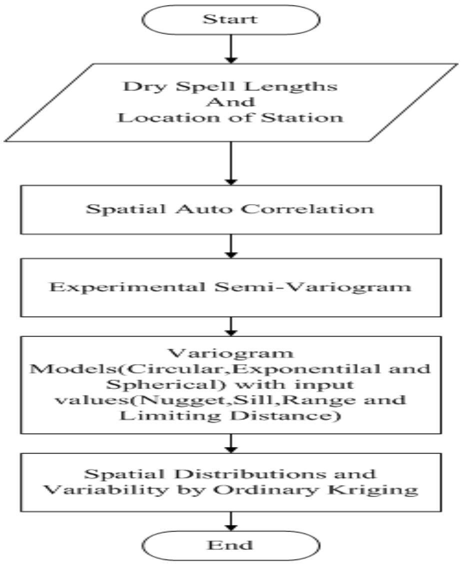

Figure 6. Flow chart in using ordinary Kriging and Gonder stations.

August and September) over Tekeze catchment showing coefficient of variability greater than 0.3. As shown in Table 3.

Temporal variability of 90th and 95th percentiles of rainfall over Tekeze river basin

The temporal variability of the 90th and 95th percentiles of rainfall over the Tekeze river basin is high with CV from 0.2 to 0.3. Very high temporal variability of the 90th and 95th percentile of rainfall is shown in northwestern station (Humera), northern station (Abiadi), northeastern stations (Edagahamus and Wukro) and southeastern station (Adigudem) with (CV>0.3).

Trend detection

The six rainfall indices at Gonder, Mekelle andEdagahamus meteorological stations having daily rainfall of period 1960-2008, 1960-2009 and 1973-2007 res-pectively were subjected to non-parametric Mann-Kendall test to detect trend. The time series of the indices only with significant trend are shown in Figures 7 to 8. The slope of each index was determined by fitting a liner regression line. The Mann-Kendall test result is shown in Tables 4. A negative trend on the 90th percentile of daily rainfall at 95% confidence interval was detected at Mekelle station as shown in Figure 7. A positive significant trend for 95th percentile of daily rainfall at Gonder station was detected as shown in Figure 8. No significant trends of the other indices were detected at Mekelle.

Dry spell length of June, July, August and September (DSLJJAS) (months of kiremt season) spatial variability over Tekeze river basin

Circular for mean dry spell length of June and mean dry spell length of August and exponential for mean dry spell length of July and spherical for the mean dry spell length of September semi variogram models are fitted. Table 5 represents the parameters that were obtained from experimental semi variogram fitting to the mean DSLJJAS data recorded at the stations in the study area and the figures with their error figures represents the interpolated spatial continuity of the DSLJJAS distributions in the catchment. Below detail interpretation of the fitted models, parameters of the models and figures with their error figures is given for their spatial variability of the DSLJJAS in the Tekeze river basin.

Interpretation of variogram models for mean DSLJJAS

The four variogram models of DSLJJAS (show a progressive decrease of spatial autocorrelation (equivalently an increase of semi-variance) until some distance (range values) in DSLJJAS in the stations in the river basin as shown in Figures 9 to 12. The dry spell length for June and August decrease their spatial dependence in circular manner in the basin but the dry spell length for July and September decrease their spatial dependence exponentially and spherically in the basin respectively. Even though the variogram models fitted to the variogram models show a common characteristics of decreasing spatial dependence with distance in the DSLJJAS in the catchment, the way they lose their spatial dependence with distance in the catchment of the four variables is different because of fitted to different variogram models with different model parameters (nugget, sill and range).

Interpretation of the nugget, sill and range values of the models of DSLJJAS

The DSLJJAS show a nugget effect in their variogram models. These nugget values of the models show two important things in the basin. The sampling interval or the lag space between the stations in the study area was taken to be 60 km because of sparse rainfall station distributions in the basin. But the nugget values in the DSLJJAS variogram models indicates the availability of few stations in the catchment basin with distance between them less than the sampling interval (60 km) and a sources of spatial variability of the variables in distance less than the sampling interval. Higher nugget value means high spatial variability of the variable less than the sampling interval. Due to this the dry spell lengths for June and September have high spatial

Table 3. Mean and CV of 90th and 95th percentiles and dry spell lengths for each months.

Variables	Station	Percentiles(mm)				Dry spell lengths (in days)							
		90th		95th		June		July		August		September	
		Mean	CV	Mean	CV	Mean	CV	Mean	CV	Mean	CV	Mean	CV
North western stations	Agibe	6.7	0.2	13.4	0.2	12.1	0.4	3.9	0.3	2.9	0.6	15.3	0.4
	Shire	9.8	0.2	17.9	0.2	5.2	0.4	2.3	0.4	2.5	0.4	6.2	0.5
	Seleklaka	9.6	0.3	17.2	0.2	9.1	0.6	2.7	0.5	3.1	0.6	11.5	0.6
	Humera	5.3	0.6	15.1	0.4	8.4	0.5	6.0	0.5	5.6	0.5	8.8	0.3
Northern stations	Aksum	6.7	0.2	14.1	0.2	10.4	0.5	3.3	0.5	4.0	0.4	10.9	0.4
	Adwa	7.5	0.2	15.1	0.2	8.5	0.5	2.3	0.6	2.4	0.4	7.6	0.5
	Abiadi	12.3	0.6	19.3	0.4	9.7	0.4	3.6	0.5	2.4	0.4	12.0	0.3
Northeastern stations	Adigrat	5.1	0.4	11.1	0.3	15.6	0.4	6.1	0.8	5.5	0.6	21.5	0.3
	Edagahamus	6.4	0.8	12.3	0.6	16.3	0.5	4.6	0.9	5.3	0.8	17.7	0.4
	Wukro	4.4	0.6	10.7	0.4	17.7	0.5	5.0	0.5	7.3	0.9	20.1	0.4
	Hawzen	4.6	0.3	10.5	0.3	16.0	0.4	3.8	0.7	4.2	0.7	18.7	0.3
	Mekelle(AB)	4.9	0.4	11.2	0.3	14.5	0.5	3.1	0.8	3.3	0.7	14.1	0.4
South Western stations	Debark	9.6	0.2	15.9	0.2	3.5	0.7	0.9	0.8	1.4	0.8	4.5	0.6
	Ambagiorgis	10.2	0.2	16.2	0.2	5.4	0.6	2.0	0.6	3.0	0.9	10.9	0.5
	Gonder	10.6	0.2	16.8	0.2	3.9	0.6	1.2	0.5	1.3	0.6	5.1	0.6
	Enfiranz	9.7	0.1	16.6	0.2	4.4	0.5	1.3	0.7	1.4	0.6	6.4	0.6
Southern stations	Lalibela	8.3	0.2	14.2	0.2	13.8	0.5	1.8	0.9	2.6	0.8	8.9	0.6
	AgereGenet	14.6	0.2	21.6	0.2	6.4	0.7	0.9	0.8	1.1	0.8	5.9	0.7
	Nifas Mewicha	9.8	0.3	16.2	0.3	9.0	0.8	3.2	0.5	2.9	0.5	6.7	0.6
Southeastern stations	Maichew	6.7	0.2	14.0	0.2	13.9	0.5	4.1	0.5	4.3	0.5	9.7	0.3
	Korem	8.4	0.3	16.6	0.2	14.4	0.4	3.6	0.4	2.9	0.3	8.2	0.6
	Adigudom	4.3	0.5	9.0	0.4	20.5	0.3	4.8	0.6	3.6	0.5	20.4	0.4
	sekota	4.9	0.3	11.8	0.2	14.2	0.4	4.4	0.3	3.7	0.5	18.6	0.4

variability in distance less than the sampling interval in the basin than the dry spell lengths in July and August. The different range values of the models in DSLJJAS show existence of spatial variability until its value in the river basin and beyond it no existence of spatial dependence of the variables in the basin. Higher range value of a variable indicates the existence of the spatial dependence of the variable of the stations separated by higher distance. Due to this all the DSLJJAS have approximately the same spatial dependence in high separated stations in the basin. The sill is the value of the variogram model attains at range. The higher the sill value of a variable, the steep becomes the model and the more rapidly changes

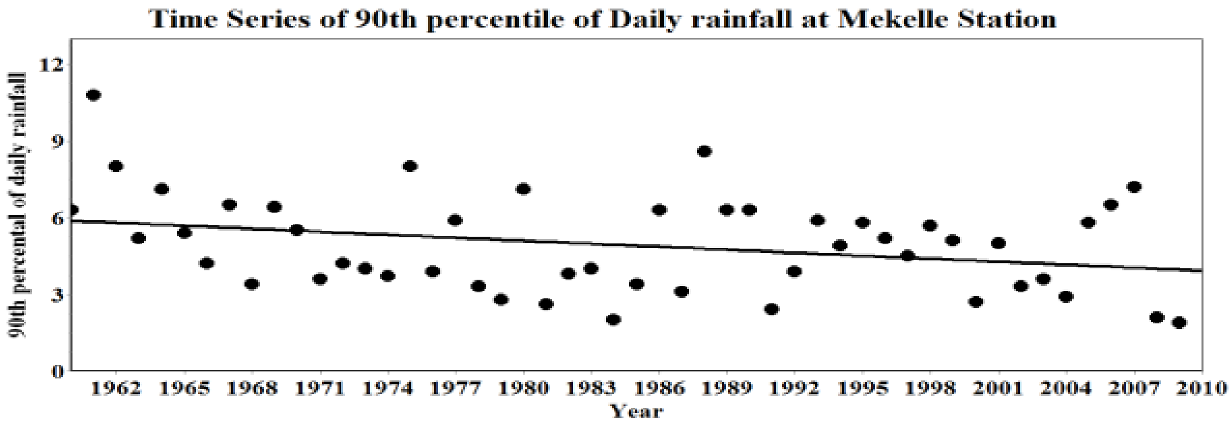

Figure 7. Time series of 90^{th} percentile with line equation of 90% = 82.65 - 0.0392 * Year at Mekelle Station.

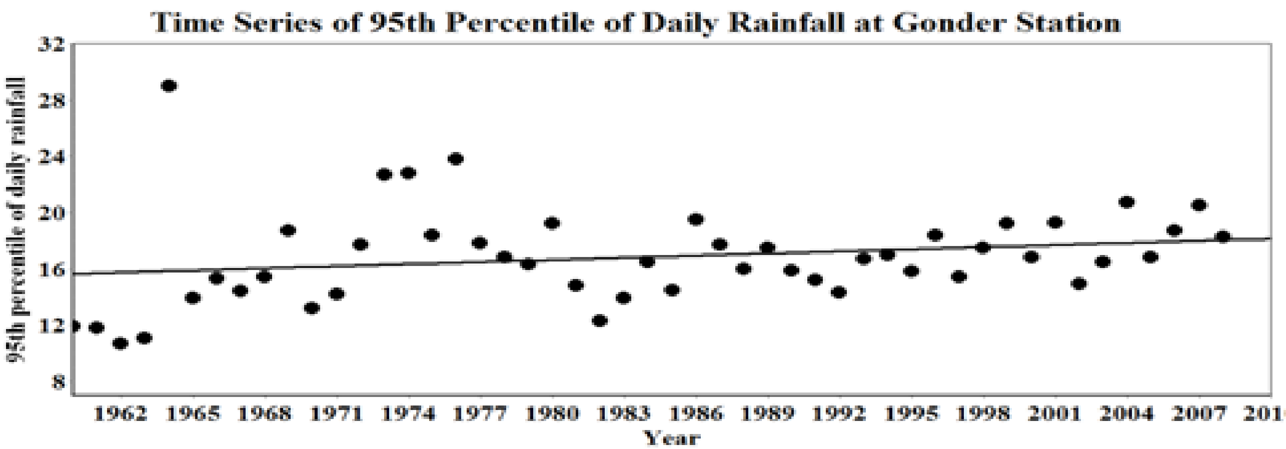

Figure 8. Time series of 95^{th} percentile with line equation of 95%=-85.57+0.0501*Year at Gonder Station.

Table 4. Mann-kendall tests.

Mann-kendall Tests for Mekelle and Gonder meteorological stations respectively					
Index name	Kendall's tau	S	P-value(Two-tailed)	alpha	Test result
90^{th}	-0.218	-267	0.026	0.05	There is trend
95^{th}	0.253	297	0.011	0.05	There is trend

Table 5. The best fitting model generated for dry spell length of June, July, August and September for the entire river basin.

Index Name	Model	Nugget	sill	Range
Dry spell length for June	Circular	4.350	31.650	239612.000
Dry spell length for July	Exponential	0.720	3.220	238818.900
Dry spell length for August	Circular	0.560	2.650	243153.100
Dry spell length for September	Spherical	5.420	34.100	250235.200

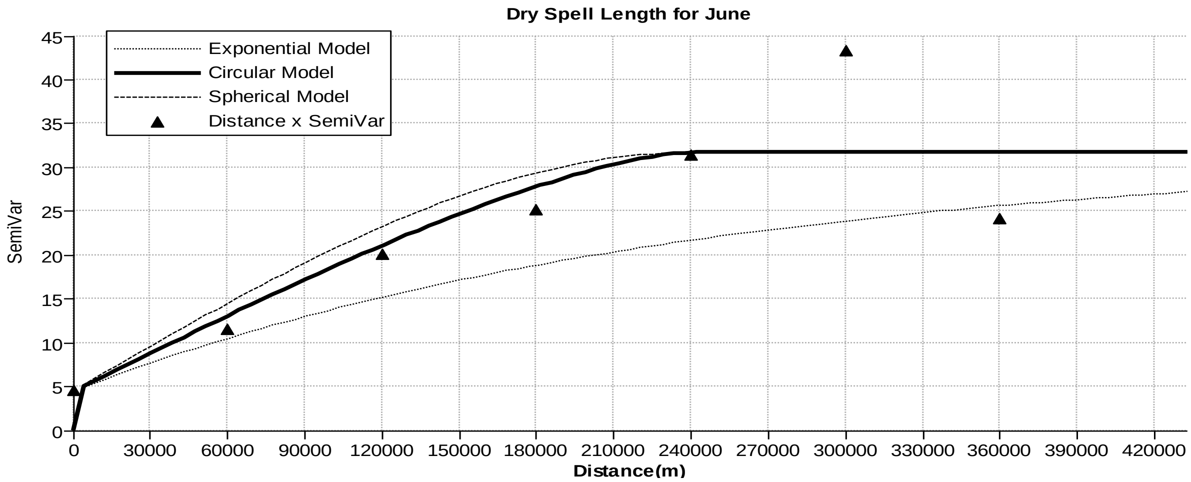

Figure 9. Circular semi variogram model fitted to dry spell length for June data set.

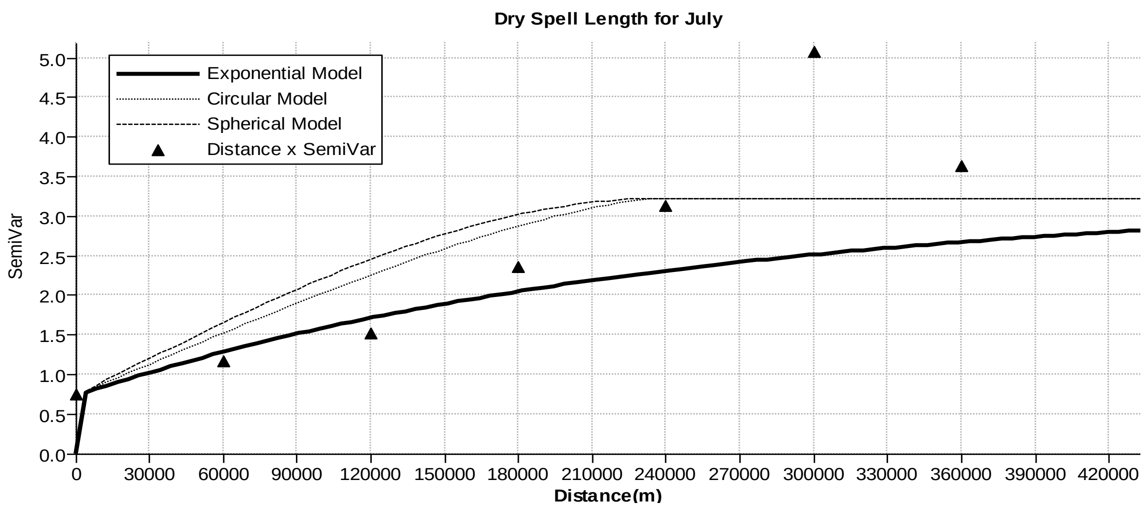

Figure 10. Exponential semi variogram model fitted to dry spell length for July data set.

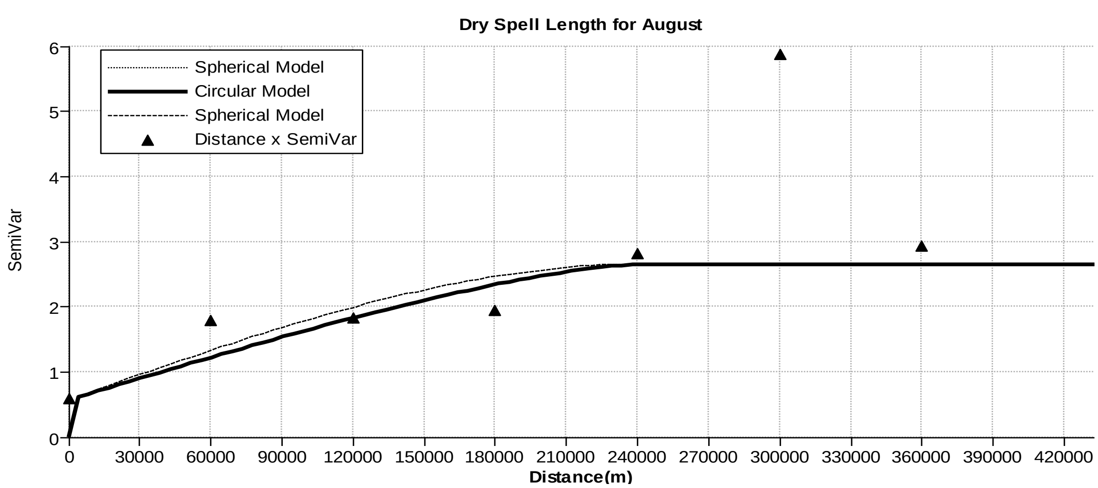

Figure 11. Circular semi variogram model fitted to dry spell length for August data set.

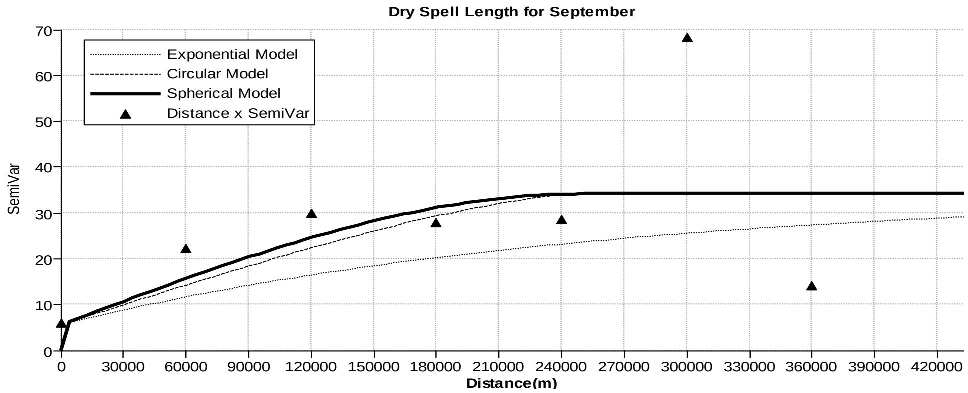

Figure 12. Spherical semi variogram model fitted to dry spell length for September data set.

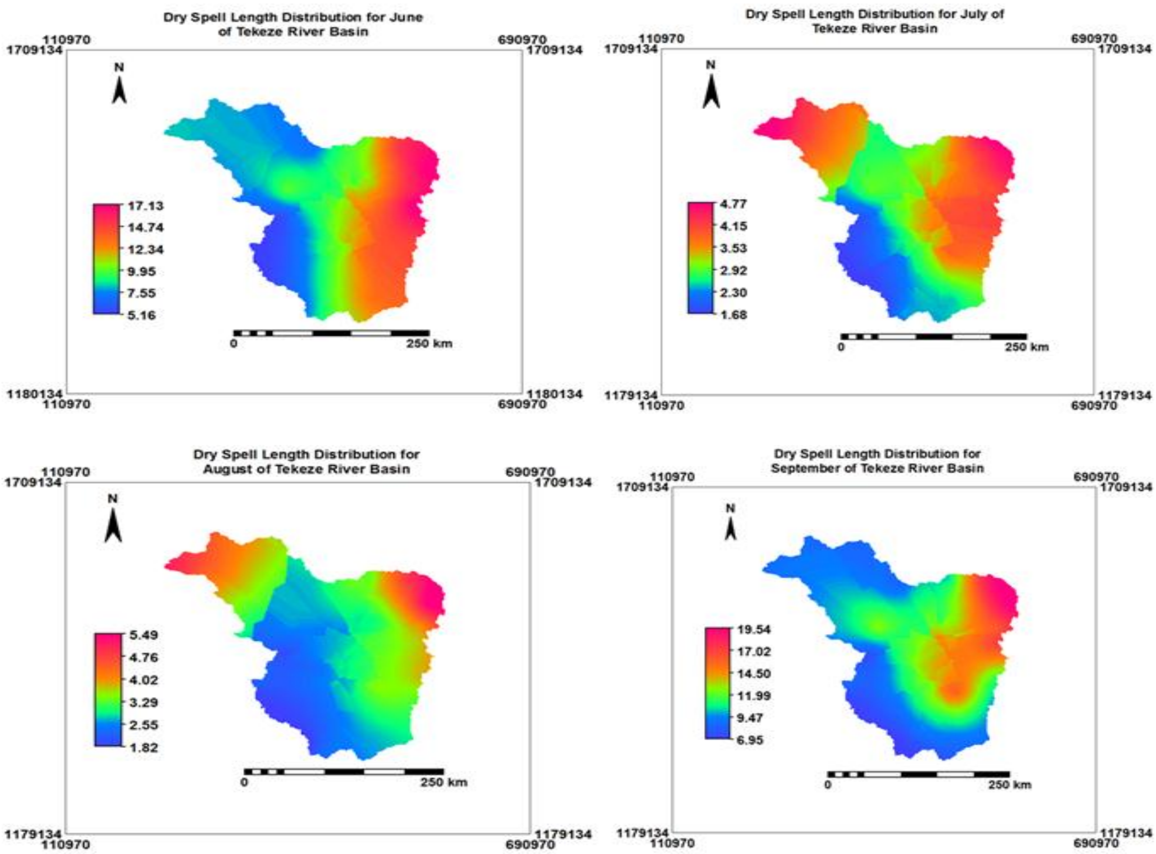

Figure 13. Spatial distribution of dry spell lengths for June, July, August and September over Tekeze river basin.

the variable in space. Because of this the dry spell lengths in June and September change more rapidly in the basin than the dry spell lengths in July and August do.

Spatial distribution estimates of DSLJJAS estimates over the river basin

The DSLJJAS figures with their error figures of the Tekeze river basin are obtained by interpolation using their fitted models by ordinary kirging. The figures of DSLJJAS indicate the spatial distribution estimates over the entire basin using the 24 stations as shown in Figure 13. The error Figure 14 of the DSLJJAS indicates the standard error of estimation of the DSLJJAS by the ordinary kirging. As indicated on the figures of DSLJJAS, the dry spell length for June varies from about 5 days in the west part of the basin to about 17 days in the east

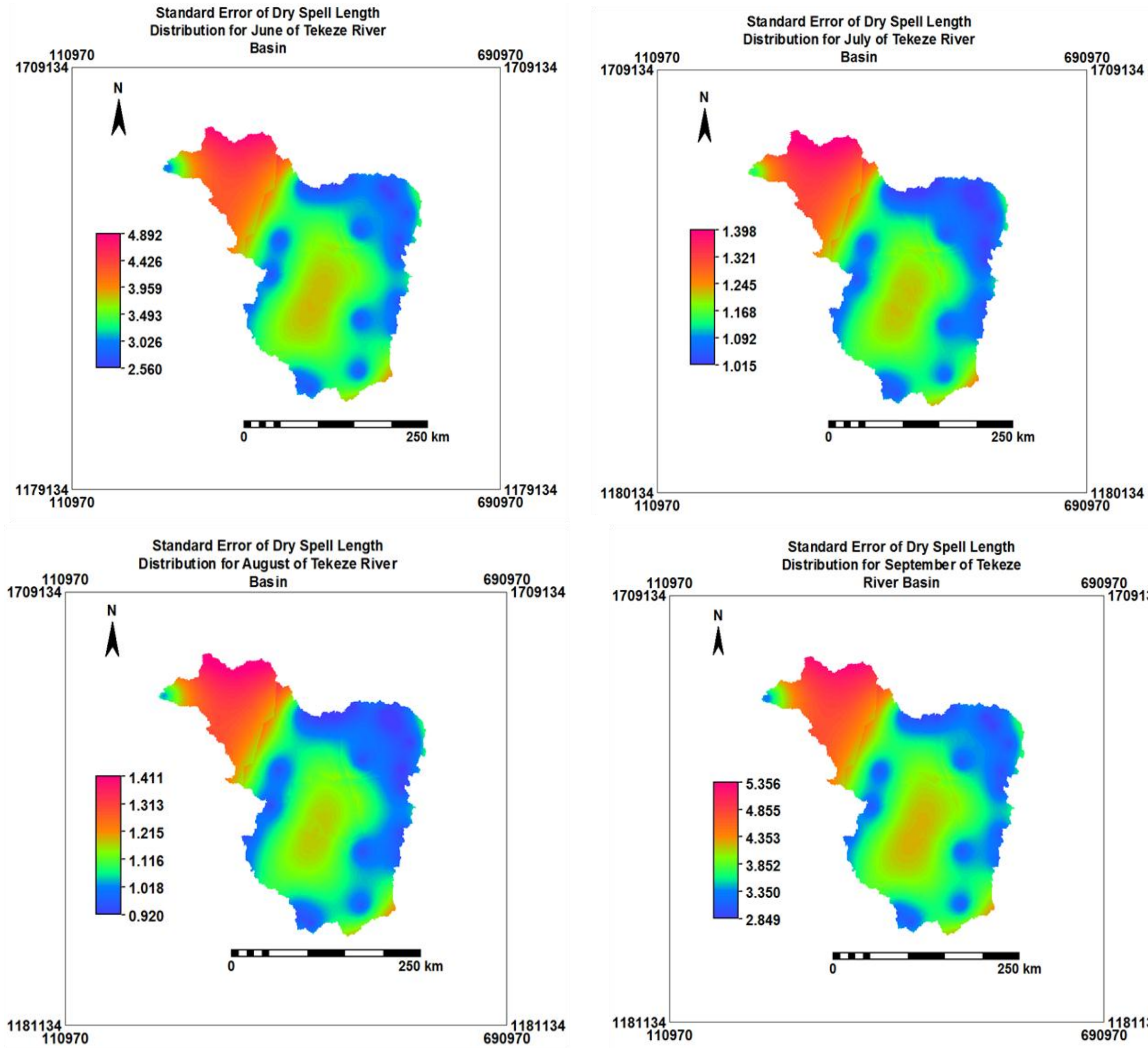

Figure 14. Standard error of spatial distribution of dry spell lengths for June, July, August and September over Tekeze river basin.

part of the basin. The dry spell length for June increases progressively from west to east part of the basin. The dry spell for July varies from about 2 days in the southwest part of the basin to about 5 days in the northwest and northeast part of the basin. South, southwest and central parts of the basin have lower dry spell length in July than other parts. The dry spell length for August varies from about 2 days in the southwest and central to about 6 days in the far northwest and far northeast parts of the basin. Dry spell length for September varies from about 7days in the south and west part of the basin to about 20 days in the northeast part. Higher standard error values in the error figure of the DSLJJAS indicate sources of spare stations in the area than the other areas. These standard errors of estimations help for decision making in the areas when the Figure 13 of DSLJJAS is used.

CONCLUSIONS AND RECOMMENDATION

The main findings of the study are summarized below. The dry spell length for the months of kiremt (June to September) season is highest in the months of June and September than the months of July and August in the Tekeze river basin. In general, the dry spell length distribution for the months of Kiremt season increases from west to east part of the river basin. There is very high year-to-year variability of dry spell length for the months of kiremt season over the basin. The dry spell lengths in June and September change more rapidly in the river basin than the dry spell lengths in July and August. A significantly decreasing trend on the 90^{th} percentiles of daily rainfall is found at Mekelle meteorological station and a significantly increasing trend on the 95th percentiles of daily rainfall is found at Gonder meteorological station.

The results, figures developed here can be very useful for meteorological, hydrological and agricultural management activities at the Tekeze river basin. Especially the information on temporal and spatial variability of dry spell lengths, are needed by the farmers on the river basin for deciding on crop types, varieties and dates for land preparations, planting and harvesting and for planning of civil and water resources projects. As in this study only 24 meteorological stations having different time periods were used, it also very important to consider world meteorological standard distributions of the stations in the basin with the same time period of data so that the result can be improved. Again the interpolation technique used in the study of the spatial variability was ordinary kirging but it is very important to do evaluation of interpolation techniques like simple kirging, co-kirging and others with ordinary kirging and choosing the best interpolation technique in the basin can improve the results.

Conflict of Interests

The authors have not declared any conflict of interests.

REFERENCES

Alexandersson H (1986). A homogeneity test applied to precipitation data. J. Climatol. 6:661-675.

Amare B (1996). Climatic resources, agro-ecological zones and farming systems in Tigray, Paper presented at the Extension Intervention Programme workshop, Mekele.18 p.

Aredo D, Seleshi Y (2003). Causes and variability of Ethiopian agriculture: modeling the relative importance of environment factors, external shocks, and state policies 1980 – 1997. In First International Policy Research Workshop in Regional and Local Development Studies onEnvironmental Management and Local Development in the Horn and East Africa, Bekure, Wolde, Semait (eds). Regional and Local Development Studies (RLDS), Addis Ababa University, 14 – 15, April 2000, Addis Ababa, Ethiopia; pp. 17-54.

Bedient PB, Huber WC (1992). Hydrology and Floodplain Analysis (New York: Addison-Wesley).

Belete K (2007). Sedimentation and Sediment Handling at Dams in Tekeze Riiver Basin, Ethiopia. PhD thesis, Norwegian University of Science and Technology, Faculty of Engineering Science and Technology, Department of hydraulic and Environmental Engineering, Trondheim, Norway.

Buishand TA (1982). Some methods for testing the homogeneity of rainfall records. J. Hydrol. 58:11-27.

Camberlin P (1997). Rainfall anomalies in the source region of the Nile and their connection with Indian summer monsoon. J. Clim. 10:1380-1392.

Ceballos A, Martinez-Fernandez J, Luengo-Ugidos MA (2004). Analysis of rainfall trends and dry period on a pluviometric gradient representative of Mediterranean climate in the Duero Basin, Spain. J. Arid Environ. 58:214-232.

Cheung WH, Senay GB, Singh A (2008). Trend and spatial distribution of annual and seasonal rainfall in Ethiopia. Int. J. Climatol. 28(13):1723-34.

Conrad V, Pollak C (1950). Methods in Climatology. Harvard University Press, Cambridge.

Degefu W (1987). Some aspects of meteorological drought in Ethiopia. In Drought and Hunger in Africa: Denying Famine a Future, Glantz M (ed.). Cambridge University Press: UK; pp. 23-36.

Göktürk OM, Bozkurt D, en ÖL, Karaca M (2008). Quality control and homogeneity ofTurkish precipitation data. Hydrol. Process. 22:3210-3218.

Gong DY, Wang JA, Han H (2005). Trend of summer dry spells in china during the late twentieth century. Meteorol. Atmos. Phys. 88:203-214.

Gonzalez-Rouca JF, Jimenez JL, Quesada V, Valero F (2001). Quality control andhomogeneity of precipitation data in the Southwest of Europe. J. Climate. 14:964-978.

Goovaerts P (1999). Performance Comparison of Geostatistical Algorithms for Incorporating Elevation into the Mapping of Precipitation. The IV International Conference on GeoComputation was hosted by Mary Washington College in Fredericksburg, VA, USA, on 25-28 July 1999.

Hurni H (1993). Land degradation, famine, and land resources scenarios in Ethiopia. In World Soil Erosion and Conservation, Pimentel D (ed.). Cambridge University Press: UK; pp. 28-61.

Michaelides SC, Tymvios FS, Michaelidou T (2009). Spatial andtemporal characteristics of the annual rainfall frequency distributionin Cyprus. Atmosph. Res. 94(4):606-615.

Novotny EV, Stefan HG (2007). Stream flow in Minnesota: Indicator of climate change. J. Hydrol. 314:319-333.

Osman M, Sauerborn P (2002). A preliminary assessments of characteristics and long-term variability of rainfall in Ethiopia-basis for sustainable land use and resources management In Conference in International Agricultural Research, Deutscher Tropentage 2002, Witzenhausen, 9-11 October.

Peterson TC, Easterling DR, Karl TR, Groisman P, Nicholls N, Plummer N, Torok S, Auer I, Boehm R, Gullett D, Vincent L, Heino R, Tuomenvirta H, Mestre O, Szentimrey T, Salinger J, Forland EJ, Hanssen-Bauer I, Alexandersson H, Jones P, Parker D (1998). Homogeneity adjustments of in situ atmospheric climate data: a review. Int. J. Climatol. 18:1493-1517.

Pettit AN (1979). A non-parametric approach to the change-point detection. Appl. Statist. 28(2):126-135

Presti R, Barca E, Parssarella G (2010). A methodology for treating missing data applied to daily rainfall in Candelaro river basin (Italy). Environ. Monit. Assess. 160:1-22.

Seleshi **Y,** Zanke **U (**2004). Recent changes in rainfall and rainy days in Ethiopia. Int. J. Climatol. 24:973-983.

Sharma TC (1996). Simulation of Kenyan longest dry and wet spells and the largest rain-sums using a Markov model. J. Hydrol. 178:55-67.

Sivakumar MVK (1992). Empirical analysis of dry spells for agricultural applicationin West Africa. J. Clim. 5:532-539.

Stern RD (1980). Analysis of rainfall at Samaru, Nigeria, using a simple two-partmodel. Arch. Meteorol. Geophys. Bioklimatol. B 28:123-135.

Tabios GQ, Salas JD (1985). A comparative analysis of techniques for spatial interpolation of precipitation. Water Resources Bulletin, 21(3):365-380.

Wolde-Mariam M (1984). Rural Vulnerability to Famine in Ethiopia: 1958-1977. Vikas: New Delhi.

International Journal of Water Resources and Environmental Engineering

Related Journals Published by Academic Journals

- *International Journal of Computer Engineering Research*
- *Journal of Chemical Engineering and Materials Science*
- *Journal of Civil Engineering and Construction Technology*
- *Journal of Electrical and Electronics Engineering Research*
- *Journal of Engineering and Computer Innovations*
- *Journal of Engineering and Technology Research*
- *Journal of Mechanical Engineering Research*
- *Journal of Petroleum and Gas Engineering*